Article

Chinese Science Bulletin

Physical Chemistry

February 2011 Vol.56 No.6: 502–507
doi: 10.1007/s11434-010-4309-7

Epitaxial growth of ultrathin ZrO_2(111) films on Pt(111)

GAO Yan, ZHANG Liang, PAN YongHe, WANG GuoDong, XU Yang, ZHANG WenHua & ZHU JunFa*

National Synchrotron Radiation Laboratory, University of Science and Technology of China, Hefei 230029, China

Received April 19, 2010; accepted August 3, 2010

Ordered epitaxial ZrO_2 films were grown on Pt(111) and characterized by low energy electron diffraction (LEED), synchrotron radiation photoemission spectroscopy (SRPES) and X-ray photoelectron spectroscopy (XPS). The films were prepared by vapor deposition of zirconium in an O_2 atmosphere followed by annealing under ultra high vacuum. At low coverages, the films grew as discontinuous two-dimentional islands with ordered structures. The size and structure of these islands were dependent on the coverage of ZrO_2 films. At coverage <0.5 monolayer (ML), $\left(\sqrt{19}\times\sqrt{19}\right)$R23.4° and (5×5) structures coexisted on the surface. As the coverage increased, the $\left(\sqrt{19}\times\sqrt{19}\right)$R23.4° structure developed with increasing degree of long-range order, while the (5×5) structure gradually faded. When the coverage reached >6 ML, a continuous ZrO_2(111) film was formed with a (1×1) surface LEED pattern coexisting with a (2×2) pattern. These ordered thin ZrO_2 films provide good model surfaces of bulk ZrO_2 and can be used for further fundamental studies of the surface chemistry of ZrO_2 using modern surface science techniques.

epitaxial growth, ordered thin ZrO_2 films, low energy electron diffraction, synchrotron radiation photoemission spectroscopy

Citation: Gao Y, Zhang L, Pan Y H, et al. Epitaxial growth of ultrathin ZrO_2(111) films on Pt(111). Chinese Sci Bull, 2011, 56: 502–507, doi: 10.1007/s11434-010-4309-7

ZrO_2 is an excellent support in the field of catalysis and has been successfully applied in many catalytic reaction systems because of its ideal chemical and mechanical stability [1–3]. However, fundamental studies on the roles of ZrO_2 in these reactions using modern surface science techniques are often hampered by charging problems because of the poor electrical conductivity of bulk ZrO_2; the band gap of ZrO_2 is approximately 5 eV [4]. In order to overcome this difficulty and further investigate the catalytic properties of ZrO_2, we adopt the commonly used method of epitaxial growth of an ordered thin oxide film on a metal single crystal surface to prepare ordered ZrO_2 thin films.

The epitaxial growth of thin ZrO_2 films has been reported on Au(111) [5], Cu(111) [6], Ag(100) [7] and Pt(111) [8–11]. A number of surface science techniques including low energy electron diffraction (LEED), scanning tunneling microscope (STM), ion scattering spectroscopy (ISS) and Auger electron spectroscopy (AES) have been used to monitor the growth of ZrO_2 films and characterize their structures. Because of the large crystal lattice mismatch, the quality and structure of ZrO_2 films varied with the substrates and were very sensitive to the substrate temperature. Maurice et al. [8] reported that ordered ZrO_2(111) films with cubic CaF_2-like structures were formed on clean Pt(111) by depositing metallic Zr at room temperature in an oxygen atmosphere followed by annealing to 900 K. They used AES and ISS to characterize the ZrO_2 films and found that ZrO_2 growth on Pt(111) followed Frank-van der Merwe mechanism (*i.e.*, layer-by-layer growth). However, following the same preparation procedure, STM analysis revealed that these films had hillock or discontinuous morphology [9]. After increasing the temperature of deposition up to 470

*Corresponding author (email: jfzhu@ustc.edu.cn)

K and post-annealing at 950 K, ordered continuous films with large terraces were obtained when the ZrO_2 thickness was >4 monolayer (ML). However, these films become discontinuous again when annealed above 1000 K.

In this paper, we investigated ordered epitaxial ZrO_2 thin films on Pt(111) surfaces using synchrotron radiation photoemission spectroscopy (SRPES), X-ray photoelectron spectroscopy (XPS) and LEED. Because of the tunability of the photon energies, SRPES can provide very surface sensitive structure information of ZrO_2 on Pt(111). Our results prove that better quality films can be obtained with a slightly higher substrate temperature for deposition than those reported in the literature [8–11].

1 Experimental

All the experiments were carried out on the surface physics endstation at beamline U18 in the National Synchrotron Radiation Laboratory (NSRL) in Hefei, China. The endstation equipment has been described in detail previously [12,13]. Briefly, the U18 beamline is connected to a bending magnet and equipped with three gratings that cover photon energies from 10 to 250 eV with a resolving power ($E/\Delta E$) > 1000. The endstation consists of chambers for analysis, preparation, and molecular beam epitaxy (MBE), with base pressures of 5×10^{-11}, 2×10^{-10} and 1×10^{-10} Torr, respectively. The analysis chamber was equipped with a VG ARUPS10 electron energy analyzer for SRPES and XPS, a twin-anode X-ray gun, retractable four-grid optics for low energy electron diffraction (LEED), and an Ar^+ sputter gun. The preparation chamber was connected with a quick load-lock port and housed a small hemispherical electron energy analyzer, an electronic gun for AES, and an Ar^+ sputter gun. The MBE chamber included a quartz crystal microbalance (QCM) for monitoring the deposition rates, a high-energy electron gun for reflection high energy electron diffraction (RHEED), and several K-cell evaporation sources.

The Pt(111) substrate (approximately 10 mm diameter × 1 mm thick) was purchased from MaTeck Company, Germany. It was cleaned, until no impurities could be detected by XPS and a sharp Pt(111)-(1×1) LEED pattern was obtained, by several cycles of Ar^+-ion sputtering, annealing at 800 K in an O_2 environment to remove carbon, and then flashing to 1300 K to remove oxygen [14]. The sample temperature was monitored by a calibrated infrared pyrometer. High-purity metallic Zr (99.99%) was evaporated at approximately 0.12 ML/min using a simple custom-built electron beam evaporator. The thin ZrO_2 films were prepared by evaporating metallic Zr onto Pt(111) under an oxygen partial pressure of 1×10^{-7} Torr at about 550 K, followed by post-annealing under the same conditions for 10 min and further annealing to approximately 1000 K without oxygen for 1 min. The annealing temperature was controlled to be no higher than 1000 K to avoid diffusion of Zr into the Pt substrate and the decay of the continuity of the film [8–11].

Taking both the photoionization cross section and grating efficiency into account, a 165 eV photon energy was used for the Pt 4f core level spectra. At this energy, the emitted electrons from Pt 4f are very surface sensitive. The valence band spectra were excited using 70 eV radiation. Before any quantitative analysis, the synchrotron radiation photoemission spectra were normalized to the photocurrents, which were measured by an Au grid located directly before the endstation. Because of the limitation of the beamline photon energy, the O 1s and Zr 3d spectra were excited using a normal X-ray source (Al Kα radiation). All the binding energies were referenced to the Fermi level of the clean Pt(111).

2 Results and discussions

2.1 Low energy electron diffraction

Figure 1 shows a group of thickness-dependent LEED patterns of the ordered epitaxial ZrO_2 films on Pt(111). On the clean Pt(111) surface, a sharp LEED pattern was observed (Figure 1(a)). After deposition of ZrO_2, the intensities of the original Pt(111) spots decreased and the background intensity increased. In addition, some new spots emerged. At a coverage of 0.4 ML, many new spots were observed around the first-order Pt(111) spots (Figure 1(b)). The same number of spots around the (0,0) spot of Pt(111) were also observed after rotating the sample so that the (0,0) spot could be seen. Analysis of this LEED pattern indicates that it corresponds to the coexistence of $\left(\sqrt{19}\times\sqrt{19}\right)$R23.4° and (5×5) structures (the latter structure was marked with white circles, as seen in the inset of Figure 1(b)). The other missing spots of these two structures are due to absence of long-range order. Meinel et al. [11] observed the (5×5) structure at a ZrO_2 coverage of 0.7 ML by STM, but did not observe it in LEED and also did not observe the $\left(\sqrt{19}\times\sqrt{19}\right)$R23.4° structure at this coverage. The $\left(\sqrt{19}\times\sqrt{19}\right)$R23.4° structure has only been reported at higher coverage (>0.8 ML [8] and >2.7 ML [11]). This indicates that under our preparation conditions these films grow two-dimensionally (2D) and parallel to the substrate with relatively larger island size. With increasing ZrO_2 thickness, the (5×5) structure attenuates, while the $\left(\sqrt{19}\times\sqrt{19}\right)$R23.4° structure increases as the degree of long-range structural order increases. At 0.8 ML coverage, the (5×5) pattern disappears and only the $\left(\sqrt{19}\times\sqrt{19}\right)$R23.4° structure is observed. At this coverage, because the Pt(111) surface is not yet fully covered by ZrO_2, the films form discontinuous 2D islands,

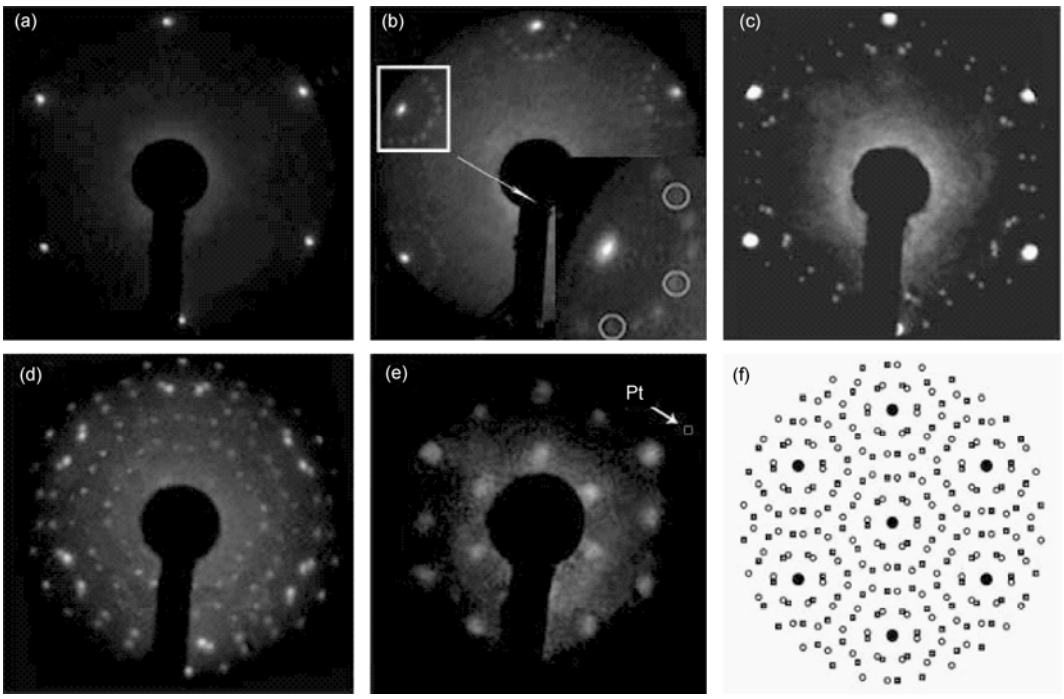

Figure 1 LEED patterns for ZrO_2 films on Pt(111) at different coverages. (a) Clean Pt (111), E = 64 eV; (b) 0.4 ML ZrO_2, E = 50 eV; (c) 0.8 ML ZrO_2, E = 55 eV; (d) 2.3 ML ZrO_2, E = 63 eV; (e) 8.3 ML ZrO_2, E = 64 eV; and (f) the schematic pattern of the $\left(\sqrt{19}\times\sqrt{19}\right)$ R23.4° structure. The inset of (b) (enlargement in white rectangle) shows new spots induced by ZrO_2 around the original Pt(111) spots. Among these new spots, the spots that belong to the (5×5) structure are marked with white circles, while the rest represents the $\left(\sqrt{19}\times\sqrt{19}\right)$ structure.

which is confirmed by SRPES (see below) and also supported by Meinel et al. [9]. Maurice et al. [8] observed a similar structure after annealing a fresh monolayer film, which was prepared at room temperature, at above 1100 K for several minutes with an oxygen partial pressure of 5×10^{-7} Torr. They assigned the structure to a $\begin{pmatrix}1.16 & 0.81\\ 0.26 & 1.37\end{pmatrix}$ incommensurate superstructure. However, after verifying the position of each spot when varying the primary electron energy, we found the spot positions matched those in the simulated $\left(\sqrt{19}\times\sqrt{19}\right)$R23.4° structure (Figure 1(f)) except for the missing spots due to lack of long-range order. Consequently, we assigned this structure to the $\left(\sqrt{19}\times\sqrt{19}\right)$ R23.4° superstructure. When the thickness of the ZrO_2 films reached 2.3 ML, a complete $\left(\sqrt{19}\times\sqrt{19}\right)$R23.4° LEED pattern was observed (Figure 1(d)). The same pattern was reported by Meinel et al. [11] after annealing a 5 ML ZrO_2 film in an O_2 atmosphere at 950 K for 1 min. This provides an additional indication that under our preparation condition, the films grow better in terms of 2D dispersion. The $\left(\sqrt{19}\times\sqrt{19}\right)$ structure is perceivable until the film thickness reaches about 6 ML, in agreement with previous results [11]. When the film is thicker than 6 ML, the surface structure evolves into a non-rotated hexagonal p(1×1) of ZrO_2(111) structure that coexists with a (2×2) pattern. In the 8.3 ML ZrO_2(111) film (Figure 1(e)) the spots of the Pt(111) substrate were no longer visible, which indicates that the films are continuous and cover the whole Pt(111) surface. Meinel et al. [9–11] and Maurice et al. [8] both observed the same structure with films prepared by different methods. Meinel et al. [9–11] obtained this surface structure after annealing a 4 ML ZrO_2 film at 980 K or a 10 ML ZrO_2 film at 950 K in 10^{-6} Torr of O_2, while Maurice et al. [8] achieved it by annealing the fresh films, which were grown at 300 K, with thickness ranging from sub-monolayer to multilayer to temperatures between 900 K and 1100 K in 5×10^{-7} Torr of O_2. According to Meinel et al. [11], charging effects appeared when the film thickness was >7 ML, which results in a significant increase in background intensity in LEED images as observed in Figure 1(e).

Considering that in the reciprocal space the nearest distance of the two spots in the Pt(111) LEED pattern corresponds to the distance between neighboring Pt atoms of the Pt crystal in real space (0.28 nm), the real space unit vectors of ZrO_2(111)-(1×1) films were calculated to be 0.359 nm from Figure 1(e). This result is in close agreement with the value of 0.36 nm reported by Meinel et al. [9–11]. Our calculated value is equivalent to the (111) planes of face

centered cubic ZrO_2 with a CaF_2-like structure [9,15]. Because of the approximately 28% lattice misfit between ZrO_2(111) and Pt(111), the (5×5) superstructure of Pt(111) observed at low coverage corresponds to the (4×4) superstructure of ZrO_2(111), as described previously [11]. The $\left(\sqrt{19}\times\sqrt{19}\right)$ superstructure of Pt(111) at medium coverage can be ascribed to the $\left(2\sqrt{3}\times2\sqrt{3}\right)$ superstructure of ZrO_2(111) [11]. For thick ZrO_2 films, the (2×2) structure of ZrO_2(111) has been assigned to a $\left(\sqrt{7}\times\sqrt{7}\right)$ reconstruction of the Pt(111) interface [11,16]. These LEED observations clearly demonstrate that the epitaxial ZrO_2 films are ordered but discontinuous at low coverage and become continuous at high coverage.

2.2 Photoelectron spectroscopy

Figure 2 shows the Pt 4f, Zr 3d and O 1s photoelectron spectra at different ZrO_2 film thicknesses. On the clean Pt(111) surface, two characteristic peaks, $4f_{7/2}$ and $4f_{5/2}$ at 71.2 and 74.5 eV, respectively, were observed in the Pt 4f region. When a ZrO_2 film is deposited on the surface, the Pt intensity attenuates gradually. At the same time, peaks related to O and Zr start to grow in the corresponding O 1s and Zr 3d regions. When the ZrO_2 thickness is <7 ML, almost no peak position shifts in Pt 4f, O 1s and Zr 3d spectra can be observed. This indicates that there is no surface charging up to this thickness, which is consistent with previous results [11]. Moreover, the peak position of Zr $3d_{5/2}$ was at a binding energy (BE) of 182.9 eV, which agrees with the literature value for Zr^{4+} (182.8 eV [8], 182.9 eV [17]). Quantitative analysis of the O 1s and Zr 3d spectra suggests that the atomic ratio of O:Zr is nearly equal to 2∶1, which indicates the formation of stoichiometric ZrO_2. When the ZrO_2 thickness is >7 ML, all the Pt 4f, Zr 3d and O 1s spectra shift to higher BE, but by different amounts. At 8.3 ML, the corresponding peak shifts are +0.2, +0.5 and +0.7 eV for Pt $4f_{7/2}$, Zr $3d_{5/2}$ and O 1s, respectively. We attributed the peak shifts to surface charging effects because of the poor conductivity, as mentioned above. The charging effects could be expected to create shifts of the same magnitude in the spectra. However, this is true only if the surfaces are uniformly exposed to the same flux and energy of incident X-rays or electrons. In the present work, the Pt 4f spectra were acquired with a phonon energy of 165 eV from synchrotron light source, different from the Zr 3d and O 1s spectra which were obtained using Al Kα (hν = 1486.6 eV) irradiation. Moreover, the Pt was directly connected to the ground. Therefore, it is expected that Pt 4f should have little or even no peak shift, while Zr 3d and O 1s should have peak shifts. The fact that Zr 3d has 0.2 eV less binding energy shift than that of O 1s may indicate that for thick ZrO_2 films Zr is probably not fully oxidized.

Note that the electron inelastic mean free path (IMAP) of Pt $4f_{7/2}$ electrons with a kinetic energy of ~94 eV passing through ZrO_2 films is about 0.66 nm [18]. In other words, if ZrO_2 grows uniformly as 2D islands up to ~6 ML (1.98 nm), the Pt $4f_{7/2}$ signal should be damped by 95%. However, the intensity of the Pt 4f peak at 6.0 ML remains approximately 10%. This indicates that at high coverages ZrO_2 films may grow discontinuously as 3D islands before the underlying 2D islands completely cover the Pt(111) surface, i.e., as a hillock mode of growth, in line with previous results observed by STM [9–11].

Figure 3 shows the valence band spectra of ZrO_2/Pt(111) with different ZrO_2 thicknesses measured with a photon

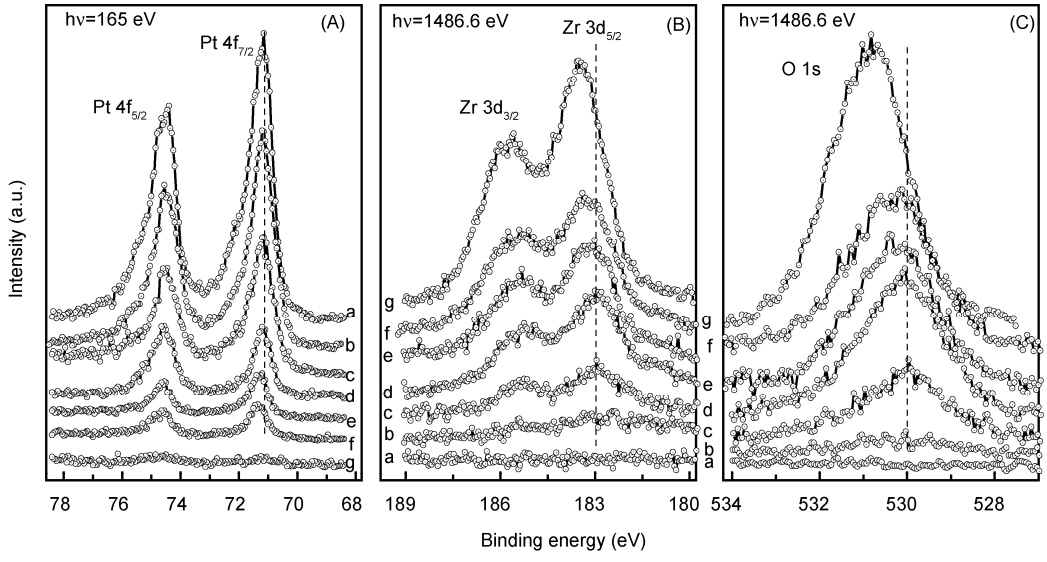

Figure 2 Spectra of Pt 4f (A), Zr 3d (B) and O 1s (C) for ZrO_2 films with different coverages. Photon energies for Pt 4f, O 1s and Zr 3d are 165, 1486.6, and 1486.6 eV, respectively. The corresponding ZrO_2 coverages are (a) 0.0, (b) 0.8, (c) 2.3, (d) 4.5, (e) 5.2, (f) 6.0, and (g) 8.3 ML.

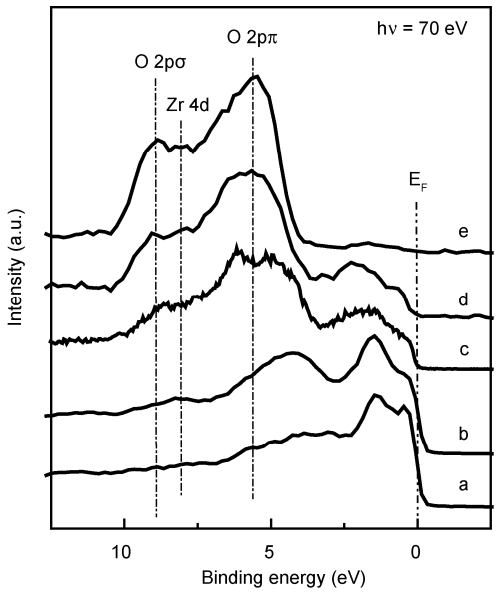

Figure 3 Valence band spectra for the ZrO_2 films grown on Pt(111). The photon energy (hν) is 70 eV. The corresponding ZrO_2 coverages are (a) 0.0, (b) 0.65, (c) 4.5, (d) 6.0, and (e) 8.3 ML.

energy of 70 eV. The bottom curve is the typical valence band spectrum from clean Pt(111), where the Pt 5d and Fermi edge are very distinct. After ZrO_2 deposition, each characteristic Pt-related signal decreases gradually in intensity, while three broad peaks at ~5.6, 8.0 and 8.8 eV, respectively, are distinguishable and gain intensity with increasing ZrO_2 thickness. The 5.6 and 8.8 eV peaks can be assigned to the nonbonding O 2pπ and bonding O 2pσ orbitals of the ZrO_2 films, respectively. This is in agreement with the calculated results of the O 2p density of states (DOS) of bulk ZrO_2, where the valence band exhibited two distinct structures at 5.67 and 8.74 eV, respectively [19]. The feature at ~8.0 eV is ascribed to the Zr 4d states [20]. When the thickness of ZrO_2 reached >6.0 ML, the valence bands of Pt could still be seen, but their intensities were considerably attenuated. In contrast, the feature between 4–10 eV appeared similar to that of bulk ZrO_2. After depositing 8.3 ML ZrO_2, the valence bands of Pt disappeared completely and the bulk ZrO_2 valence band feature was observed, which is indicative of the formation of bulk ZrO_2 on the surface. At the photon energy of 70 eV, the photoionization section of O 2p is three times larger than that of Zr 4d. Therefore, the valence band of the ZrO_2 films is dominated by the O 2p character, and only a small Zr 4d contribution can be seen, which is similar to other oxides like HfO_2 [21]. With an excitation energy of 70 eV the electrons from the valence band of Pt have kinetic energies that fall into the valley region of the universal curve, and they represent the surface sensitive information. Considering the IMAP of these electrons is only approximately 0.6 nm [18], the observation of a clear valence band for Pt at ZrO_2 thickness >4.5 ML (1.48 nm) again suggests the formation of 3D ZrO_2 islands before they coalesce into 2D uniform films to cover the substrate Pt(111) surface completely. Only at higher coverage does the deposited ZrO_2 become a continuous film on Pt(111). These valence band results agree with the aforementioned Pt 4f and LEED results.

From these results, it is clear that compared with the film obtained by Meinel et al. [9–11] the ZrO_2 film grows better by 2D dispersion under our preparation conditions, especially at low coverage values. Obviously, the preparation conditions affect the growth of ZrO_2 film. Meinel et al. [9] grew ZrO_2 films at substrate temperatures of 300 and 470 K, and found that an increased substrate temperature improved the film quality. In addition, the post-annealing temperature was also critical to the film growth. When the ZrO_2 films grown at 470 K were post-annealed in oxygen environments at 950 K, STM analysis revealed smoother film morphologies than after post-annealing at 900 K [9]. However, as discussed previously [9], increasing the post-annealing temperature to about 1050 K did not yield the desired completely smooth film, but instead induced discontinuity of the films. Based on these investigations, we hypothesized that further increases in the substrate temperature during film growth would improve the film quality. Consistent with this hypothesis, increases in the Pt(111) sample temperature to 550 K resulted in larger 2D ZrO_2 islands. Therefore, the substrate temperature is an important parameter for ZrO_2 film growth on Pt(111). However, when the substrate temperature was increased to be >600 K for the film growth, the ZrO_2 superstructure spots in the LEED images became blurred (results not shown), which indicates the film quality is reduced. This is probably caused by ZrO_2 film agglomeration on Pt(111) because the interaction between the film and substrate is relatively weak, as found in DFT calculations [10,11].

Meinel et al. [10] observed a growing carbon signal in the low ZrO_2 coverage region when the film was discontinuous. They claimed that this growing C contamination was not observed for continuous ZrO_2 film. However, in the present study, we did not observe carbon contamination during the entire process of ZrO_2 growth. This may also be partially responsible for a better quality of the films presented here compared with those of Meinel et al.

3 Conclusions

Ordered epitaxial ZrO_2(111) films were grown on Pt(111) with sub-monolayer to multilayer coverage. These films were of better quality and grown using a slightly different preparation method than those previously reported [8–11]. The surface structures of the ordered ZrO_2 films varied with the film thickness. At low coverages, the films were discontinuous, and the degree of long-range order increased as the film thickness increased. At high coverage, a continuous fcc crystalline structure similar to bulk ZrO_2 formed with the (111) plane parallel to the substrate Pt(111) plane. These

ordered thin ZrO_2 films could be used as model surfaces for further studies of the surface properties of bulk ZrO_2.

We would like to thank Dr. G. Held (Reading University, UK) for his helpful discussions on the LEED results. This work was supported by the Specialized Research Fund for the Doctoral Program of Higher Education (SRFDP, 200803580012), the National Natural Science Foundation of China (20873128), the Program for New Century Excellent Talents in University (NCET), the National Basic Research Program of China (2010CB923302) and the Hundred Talents Program of the Chinese Academy of Sciences.

1 Zhang X, Shi H, Xu B Q. Comparative study of Au/ZrO_2 catalysts in CO oxidation and 1,3-butadiene hydrogenation. Catal Today, 2007, 122: 330–337
2 Fujii H, Mizuno N, Misono M. Pronounced catalytic activity of $la_{1-x}Sr_xCoO_3$ highly dispersed on ZrO_2 for complete oxidation of propane. Chem Lett, 1987, 16: 2147–2150
3 Idakiev V, Tabakova T, Naydenov A, et al. Gold catalysts supported on mesoporous zirconia for low-temperature water-gas shift reaction. Appl Catal B, 2006, 63: 178–186
4 Kralik B, Chang E K, Louie S G. Structural properties and quasiparticle band structure of zirconia. Phys Rev B, 1998, 57: 7027–7036
5 Lou J R, Hess U, Mitchell K A R. The growth of zirconium-oxide thin-films on Au(111) single-crystal surfaces. Appl Surf Sci, 1992, 62: 175–180
6 Paulidou A, Nix R M. Growth and characterisation of zirconia surfaces on Cu(111). Phys Chem Chem Phys, 2005, 7: 1482–1489
7 Meinel K, Schindler K M, Neddermeyer H. Scanning tunneling microscopy study on the preparation and characterization of zirconium oxide islands on Ag(100). Surf Sci, 2002, 515: 226–234
8 Maurice V, Salmeron M, Somorjai G A. The epitaxial-growth of zirconium-oxide thin films on Pt(111) single-crystal surfaces. Surf Sci, 1990, 237: 116–126
9 Meinel K, Schindler K M, Neddermeyer H. Growth, structure and annealing behaviour of epitaxial ZrO_2 films on Pt(111). Surf Sci, 2003, 532: 420–424
10 Meinel K, Eichler A, Schindler K M, et al. STM, LEED, and DFT characterization of epitaxial ZrO_2 films on Pt(111). Surf Sci, 2004, 562: 204–218
11 Meinel K, Eichler A, Forster S, et al. Surface and interface structures of epitaxial ZrO_2 films on Pt(111): Experiment and density-functional theory calculations. Phys Rev B, 2006, 74, 235444
12 Zhao W, Guo Y X, Feng X F, et al. Electronic structure and chemical reaction of Ca deposition on regioregular poly(3-hexylthiophene) surfaces. Chinese Sci Bull, 2009, 54: 1978–1982
13 Zhu J F, Bebensee F, Hieringer W, et al. Formation of the calcium/poly(3-hexylthiophene) interface: Structure and energetics. J Am Chem Soc, 2009, 131: 13498–13507
14 Zhu J F, Kinne M, Fuhrmann T, et al. *In situ* high-resolution XPS studies on adsorption of NO on Pt(111). Surf Sci, 2003, 529: 384–396
15 Jensen J A, Rider K B, Chen Y, et al. High pressure, high temperature scanning tunneling microscopy. J Vac Sci Technol B, 1999, 17: 1080–1084
16 Eichler A. Modeling oxide-metal interfaces from density-functional theory: Platinum adsorption on tetragonal zirconia. Phys Rev B, 2003, 68: 205408
17 de González C O, García E A. An X-ray photoelectron spectroscopy study of the surface oxidation of zirconium. Surf Sci, 1988, 193: 305–320
18 Seah M P, Dench W A. Quantitative electron spectroscopy of surfaces: A standard data base for electron inelastic mean free paths in solids. Surf Interface Anal, 1979, 1: 2–11
19 Morant C, Fernandez A, Gonzalez-Elipe A R, et al. Electronic structure of stoichiometric and Ar^+-bombarded ZrO_2 determined by resonant photoemission. Phys Rev B, 1995, 52: 11711–11720
20 French R H, Glass S J, Ohuchi F S, et al. Experimental and theoretical determination of the electronic-structure and optical-properties of 3 phases of ZrO_2. Phys Rev B, 1994, 49: 5133–5141
21 Bersch E, Rangan S, Bartynski R A, et al. Band offsets of ultrathin high-kappa oxide films with Si. Phys Rev B, 2008, 78: 085114